Report no. changed (Mar 2006): SM-399-UU

SACLANT UNDERSEA RESEARCH CENTRE REPORT

SACLANTCEN MEMORANDUM
serial no: SM- 399

Project 03F - 1: Phase I Completion report

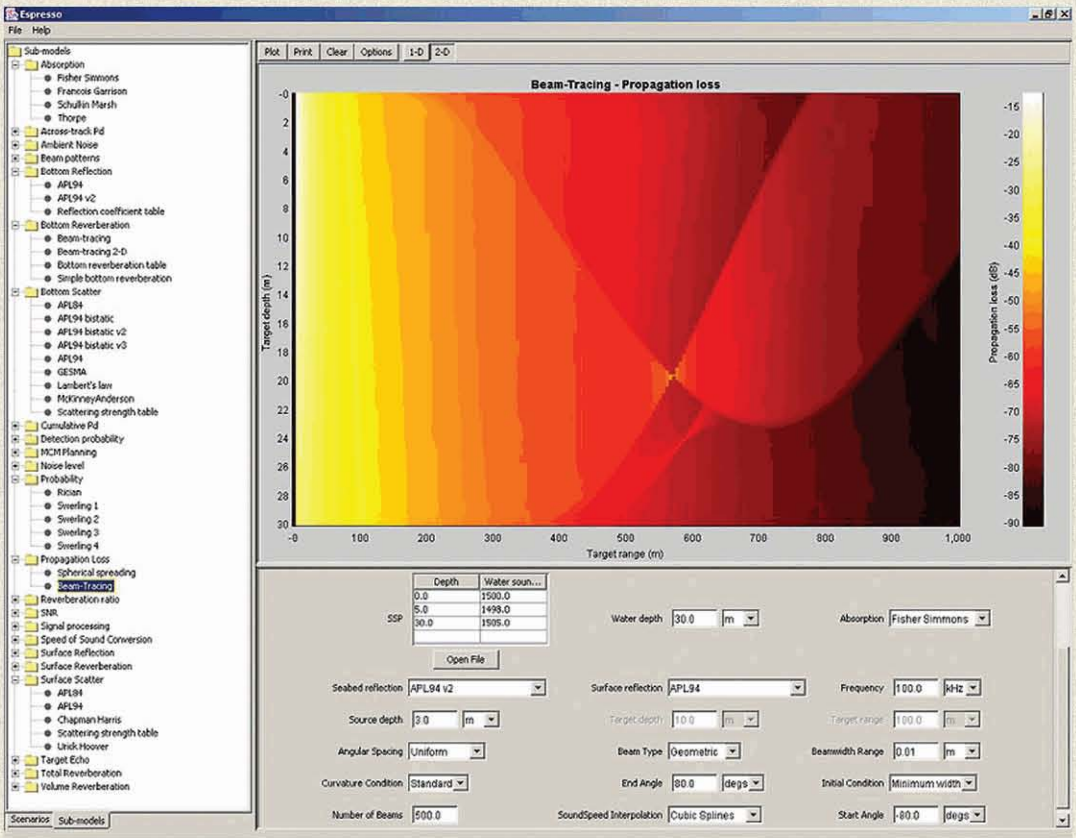

Gary L. Davies

December 2002

NORTH ATLANTIC TREATY ORGANIZATION   ORGANISATION DU TRAITE DE L'ATLANTIQUE NORD

Report no. changed (Mar 2006): SM-399-UU

03F-1 Phase I Report

G. L. Davies

The content of this document pertains to work performed under Project 03F-1 of the SACLANTCEN Programme of Work. The document has been approved for release by The Director, SACLANTCEN.

Jan L. Spoelstra
Director

intentionally blank page

03F-1 Phase I Report

G. L. Davies

Executive Summary: Trials conducted over several years with the NATO Immediate Reaction Forces have demonstrated that Command Teams experience problems in quantifying minehunting sonar performance, especially in areas where the environmental factors combine with low target strength mines to produce difficult minehunting conditions. Inexact performance predictions result in poor evaluations of mine clearance which in turn lead to inaccurate assessments of remaining risk to follow-on forces in the channel or area.

Project 03F-1 is developing a standard NATO minehunting sonar performance assessment tool (ESPRESSO) that will interface directly with the NATO MCM planning and evaluation tactical decision aids (e.g. MCM EXPERT) to improve planning and evaluation methods to cover every type of minehunting operation. This tool will provide accurate sonar performance predictions to enhance the safety of NATO forces conducting MCM operations and to improve NATO MCM C4I.

This report describes work carried out during Phase I of Project 03F-1. The main tasks carried out during this phase were: survey of models; development of essential sub-models; and software prototyping. The report also summarizes the tasks that will need to be carried out during the remainder of the project to complete the development and validation of ESPRESSO.

intentionally blank page

03F-1 Phase I Report

G. L. Davies

Abstract: This report describes the results of Phase I of Project 03F-1. The overall aim of this project is to develop and validate a NATO minehunting sonar performance assessment tool that will be capable of not only providing Signal-to-Noise ratio versus range, but also converting these data to a detection probability (both single ping and multiple integrated pings) and the cumulative detection probabilities required by the minehunting tactical models (lateral range curves).

Phase I of this project covered the following tasks: survey of existing models; software prototyping; and development of algorithms.

Keywords: MCM ∘ minehunting ∘ sonar performance ∘ reverberation

Contents

1 Introduction

This report describes Phase I of Project 03F-1. The main aim of this project is to develop a standard NATO minehunting sonar performance assessment tool that will interface directly with the NATO MCM planning and evaluation tactical decision aids such as MCM EXPERT. This tool has been named ESPRESSO (Extensible Performance and Evaluation Suite for Sonar). Figure 1 shows the interfaces to ESPRESSO, the main inputs being the environmental, sonar, and target parameters, and the main outputs being the planning parameters required by MCM planning tools. The input parameters could come from a variety of sources such as national or NATO databases, ship sensors and, in the case of environmental data, from Rapid Environmental Assessment (REA).

Phase I of this project covered the following tasks:

- Survey of existing models
- Development and implementation of algorithms
- Software prototyping

The survey of existing models was done to ensure that work already carried out by the nations was not repeated unnecessarily by the project. Following the survey it was possible to identify those algorithms that needed to be developed and implemented.

A primary goal of the project was to produce a tool that would allow new sub-models

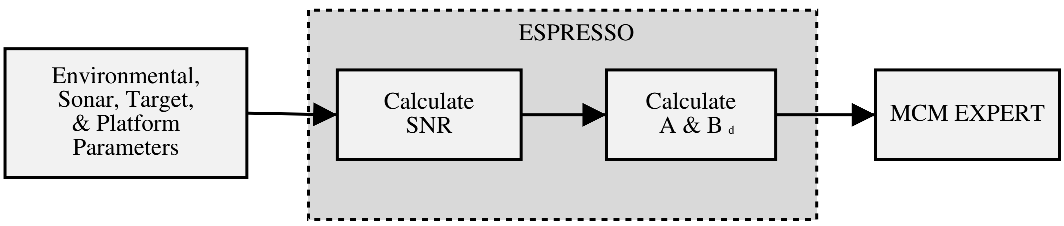

Figure 1 *Interfaces to ESPRESSO*

to be added without requiring changes or recompilation of the existing code. This approach has the following advantages:

- Sub-models can be easily updated
- New functionality can be added easily by adding new sub-models
- Nations can replace sub-models with their own classified sub-models
- The user interface can be customized for different sonar systems

Since it was not clear at the outset of the project how this goal could be technically achieved, software prototyping was used to find a technical solution.

There are two further phases to the project. In Phase II, taking the prototype software developed during Phase I as a starting point, a beta version of ESPRESSO will be designed and implemented that is suitable for use by military users. In Phase III, ESPRESSO will be tested by comparing results from ESPRESSO with the results of Percentage Clearance (PC) trials and with measured data collected by SACLANTCEN.

2
Survey of models

A survey was done primarily to see whether any existing models satisfied, or partially satisfied, the principle requirements for a NATO minehunting performance prediction model. These requirements are:

- Contains up-to-date algorithms
- Provides the inputs required for MCM planning tools
- Is releasable within NATO

The aim was to avoid replication of work already done within nations by basing the NATO model on an existing national model. A number of visits were made to government laboratories and industry as a part of the survey of existing models. Amongst the models surveyed were:

- MINERAY3 (ARL, University of Texas, US)
- PC SWAT (CSS, Panama City, US)
- CASS (NUWC, Division Newport, US)
- HUNTOP (TNO, The Hague, NL)

These models are all based on propagation models using ray tracing or Gaussian beam tracing and which include multipaths. (CASS includes a propagation model called GRAB [15].) For all these models the biggest hurdle was releasability within NATO — an essential requirement. There were, initially, indications that CASS might be releasable and it was originally planned to base the tool produced by the project on CASS. Since CASS contains state-of-the-art acoustic sub-models it would have provided, with the addition of algorithms for the MCM planning inputs and a user interface, a suitable basis for a NATO minehunting performance prediction tool. However, permission was not obtained to release CASS within NATO and the result of the survey was that no models were found that would be suitable as a basis for the NATO minehunting performance prediction model.

The implications of not being able to use CASS as the basis of the NATO model were both positive and negative. Use of CASS as the basis of ESPRESSO would have made it impossible to achieve the goal of being able to add new algorithms easily without changing existing code. However, the unavailability of CASS placed the extra burden on the project of developing a suitable reverberation model (described in section 3.2).

3 Sub-models

A set of sub-models was implemented during Phase I in order to allow prediction of target echo to background ratio. Although all the sub-models that are essential to the prediction of target echo to background ratio have been implemented, other sub-models are expected to be added over time both within Project 03F-1 and by other projects at SACLANTCEN. Since most of these sub-models are described in other reports and journals, references to these are given rather than duplicating information in this report.

3.1 Propagation sub-model

A modified version of BELLHOP, a public-domain ray/beam model by Porter [29], has been used for the propagation sub-model. The original code has been modified to allow calculation of reverberation [24, 26] and has been re-written in the Java programming language. The code implements a robust variant of Gaussian beam tracing [30] known as geometric beam tracing [17]. Beam methods continue to be especially attractive for active sonar modelling, as they are well suited for high-frequency problems, range dependent environments, and broadband sources. In contrast to full wave models, the computation of propagation paths and travel times is independent of frequency, other than the frequency-dependent absorption coefficient. The geometric beam approach reconstructs the ray-theoretical result and therefore is unsuitable for use at very low acoustic frequencies. This technique is far more computationally efficient and more robust than more traditional eigenray finding techniques. This version of BELLHOP allows propagation loss to be calculated as acoustic intensity in two dimensions (range and depth).

3.2 Reverberation sub-models

Reverberation sub-models have been implemented for sea surface, sea bottom, and volume (water column) reverberation [25]. These sub-models are applicable to monostatic sonar geometries and narrow bandwidths. For wide-band sonars, it may be necessary to run the sub-model several times for frequencies sampled over the sonar bandwidth and then to average the results over frequency.

For the sea surface and sea bottom reverberation sub-models, the sea surface and bottom are spatially sampled using a line of equally spaced scatterers running outwards from the source at the sea surface and seabed respectively. In the case of the volume reverberation sub-model, the water column is spatially sampled using a grid of scatterers. For each scatterer a series of eigenrays is calculated using the propagation sub-model. The reverberation intensity is calculated for each combination of eigenrays from the source to a scatterer and back again. The resulting reverberation intensity is added to a time bin, depending on the two-way travel time. The final result of each of the reverberation sub-models is reverberation intensity as a function of two-way travel time.

3.3 Target echo sub-model

There are some similarities between the reverberation sub-models [25] and the target echo sub-model. However, rather than a line (or grid) of scatterers there is a single target position with an associated target strength (as opposed to scattering strength). As for the reverberation sub-models, the resulting target echo intensity for each combination of eigenrays from the target to the sonar is added to a time bin, depending on the two-way travel time. The size of the time bins is important since, depending on the size of the time bin, the target echo from more than one path may contribute to a given time bin, affecting the target echo level. The time bin size should normally be equivalent to the time resolution of the sonar. This sub-model is applicable to mono-static sonar geometries and narrow bandwidths.

In general, this sub-model is used to calculate target echo intensity as a function of target range or depth. The value of target echo intensity for a given target position, x, is then given by the maximum target echo intensity over time for that target position, i.e. $EL_x = \max(EL_{x,t1}, EL_{x,t2}, EL_{x,t3}, \ldots, EL_{x,tn})$, where $EL_{x,t1}$ is the echo intensity for a target at position x at time $t1$.

3.4 Signal to background ratio sub-model

The signal to background ratio is defined here as the ratio of the target echo intensity to the reverberation plus noise intensity. In this sub-model, the signal to background ratio for a given target is calculated as a function of travel time by dividing the target echo intensity as a function of time by the total background intensity (total reverberation plus noise) as a function of time. Target echo intensity, reverberation intensity, and noise intensity are calculated using the sub-models described elsewhere in this section.

As for the target echo sub-model, this sub-model is generally used to calculate signal to background ratio as a function of target range or depth, rather than as a function of time for a single target position. In this case, the signal to background ratio for a target at position x is given by the maximum signal to background ratio over time corresponding to that target position, i.e.

$$SNR_x = \max\left(\frac{EL_{x,t1}}{BL_{t1}}, \frac{EL_{x,t2}}{BL_{t2}}, \ldots, \frac{EL_{x,tn}}{BL_{tn}}\right)$$

where SNR_x is the signal to background ratio for a target at position x, and BL_{t1} is the background intensity at time $t1$.

3.5 Other acoustic sub-models

Absorption Coefficient Four sub-models have been implemented for calculating the absorption coefficient in water: Fisher-Simmons [12]; Francois-Garrison [2, 13]; Schulkin-Marsh [32]; and Thorp [34]. The algorithm recommended by APL-UW [2] is Francois-Garrison in which the constants in the equation have been fitted to many oceanic measurements. In most environments Francois-Garrison and Fisher-Simmons, which is based on laboratory experiments, give very similar results. However, at high frequencies and in warm water, Francois-Garrison gives much higher values for the absorption coefficient than Fisher-Simmons. According to Edgecock [11] it is Francois-Garrison that is incorrect in this regime. For this reason, Fisher-Simmons is the default sub-model for the absorption coefficient in ESPRESSO. Schulkin-Marsh and Thorp have been included for convenience when comparing with other models that use them, but they are not recommended.

Surface Forward Loss Only one surface forward loss sub-model has been implemented, that from APL-UW 1994 [9, 35]. This sub-model has been validated by acoustic measurements made in the frequency range 20–50 kHz and is recommended for reverberation calculations in the APL-UW 1994 report [2] for frequencies between 10–100 kHz. This sub-model is recommended for use when the vertical beamwidth is greater than approximately 20° and the horizontal beamwidth is greater than approximately 5° since, under these conditions, the angular spreading of the reflected energy can be ignored.

Surface Backscatter Four sub-models have been implemented for calculating surface backscattering strength: APL-UW 1994 [2, 8, 20, 21]; Chapman-Harris [5]; APL-UW 1984 [1]; and Urick-Hoover [36]. The default sub-model in ESPRESSO is the APL-UW 1994 sub-model in which the backscattering from near-surface bubbles is calculated, this being the dominant scattering mechanism at high frequencies. The APL-UW 1994 sub-model is applicable over the frequency interval of 10–100 kHz. The other sub-models are included for convenience, but are not recommended. The bistatic surface scattering model by

Dahl [10] using the small slope approximation may be implemented in the future. This could potentially give more accurate results than the APL-UW 1994 algorithm.

Bottom Forward Loss The bottom forward loss sub-model is a simple physics-based model first published by Mackenzie [2, 18] in which the Rayleigh reflection coefficient is modified by using a complex wavenumber in the sediment to take account of attenuation. This sub-model is recommended in the APL-UW 1994 report [2]. Losses due to scattering are not currently included.

Bottom Backscatter Five bottom backscatter sub-models have been implemented: APL-UW 1994 [2, 28]; APL-UW 1984 [1]; McKinney-Anderson [22]; GESMA [4]; and Lambert's law [19]. By default, ESPRESSO uses the bottom bistatic scatter sub-model rather than any of the backscatter sub-models. The most recent of the backscatter sub-models is the APL-UW 1994 model which is, in part, physics-based. The McKinney-Anderson algorithm is a fit by ARL:UT to averages of data collected by McKinney-Anderson over a frequency range of 12.5 kHz to 290 kHz dating back to the 1960s.

Bottom Bistatic Scatter The APL-UW 1994 [2] algorithm has been implemented and is the default bottom scatter sub-model in ESPRESSO. This is a generalization of the APL-UW 1994 backscatter model. The bistatic version uses the perturbation approximation (except near specular geometries, where the Kirchhoff approximation is used) rather than the composite roughness approach used in the backscatter model. The algorithm is stated as being applicable for frequencies between 10–100 kHz [2].

Improvements to this sub-model, such as the use of the small slope approximation, will be incorporated when they become available. Other improvements in the estimation of bottom scattering strength are planned to come from work being carried out in Project 03H-1 at SACLANTCEN. In particular, it is hoped that the statistics of bottom reverberation can be provided in addition to the mean level. Using more realistic statistical distributions than the usual Rayleigh distribution should improve the accuracy of the calculation of probability of detection.

Ambient Noise The implemented algorithm is a fit to the widely used Knudsen [16] curves. The algorithm includes rain noise [14] and thermal noise. The APL-UW 1994 [2] sub-model, which takes into account the directionality of noise, is likely to be implemented in the future since it should give greater accuracy.

Biological Noise No algorithms have been implemented, so far, for biological noise. The APL-UW 1994 report [2] contains data but no algorithms for biological noise. Algorithms for biological noise may be added when they become available.

Receiver Noise Receiver noise is not currently included, but this will be a simple addition to ESPRESSO which will be included in the next phase of the project.

Platform Noise There is currently no algorithm implemented. A lookup table is likely to be provided for nations to input their own data. This will be implemented during the next phase of the project.

Speed of Sound The Chen-Millero-Li [6, 7, 27] algorithm has been implemented. This is recommended in APL-UW 1994 [2] for its range of validity and accuracy.

3.6 Mine-case burial prediction

Three sub-models have been implemented for the prediction of mine-case burial. One of these, DRAMBUIE [33], was developed by the UK for prediction of mine-case burial due to scour. The two other sub-models predict mine burial due to liquefaction based on the work of Sakai et al. [31]. A description of these sub-models together with the results of a trial designed to validate them can be found in the final report of the NATO Sub-Group 31 [33]. The final report stated that there was general agreement between predictions of scour and observations during the trial but, since mine burial due to liquefaction did not occur, the liquefaction sub-models could not be checked. Sub-models to predict mine-case burial due to other mechanisms such as impact, gravity sinking, shakedown, bed-form migration, and sedimentation are not currently available. If and when new models become available they can be incorporated into ESPRESSO, but it is not intended to develop any mine-case burial sub-models within Project 03F-1. (A look-up table exists for impact burial based on results from a US model, this may be included in ESPRESSO in the future.) The releasability of these sub-models to NATO nations that were not participants of NATO Sub-Group 31 needs to be confirmed.

A simple sub-model to predict the reduction in target strength due to mine-case burial (either full or partial) developed by Fox [33] has been implemented. However, it is planned that the results of Project 03E-2 at SACLANTCEN will be used to implement a more sophisticated target sub-model for both buried and proud mines.

4

Inputs to MCM planning

MCM planning tools, such as MCM EXPERT, require sonar performance to be described as either a lateral range ($P(y)$) curve (section 4.3) or as A and B_d values (section 4.4). The lateral range curve defines the probability of detecting a target as a function of lateral distance from the ship's track. The A and B_d values characterize the lateral range curve: A is known as the characteristic detection width and characterizes the width of the curve; B_d is know as the characteristic probability of detection and characterizes the height of the curve. The values are derived from the signal to background ratio: first by calculating a single-look probability of detection (section 4.1) and then deriving the cumulative probability of detection (section 4.2).

4.1 Probability of detection

The equations implemented for calculating probability of detection were derived by Swerling in the early 1950s for various types of fluctuating radar targets. Swerling defines four cases for fluctuating targets:

Case 1 For targets consisting of many independent scatterers where the target fluctuates slowly with respect to the pulse repetition rate.

Case 2 For targets consisting of many independent scatterers with pulse-to-pulse fluctuations of a Rayleigh nature.

Case 3 For targets with a single dominant scatterer with no pulse-to-pulse fluctuations.

Case 4 For targets with a single dominant scatterer with pulse-to-pulse fluctuations.

For sonar systems, where the pulse repetition rates are far lower than for radar systems, cases 1 and 3 are probably not appropriate. For a typical mine-like target, insonified by a high-resolution minehunting sonar, case 2 is probably the most appropriate since these targets tend to have scatterers distributed over their surface. For a simple spherical or cylindrical target, case 4 may be more appropriate. The equations for the Swerling cases are taken from Meyer-Mayer [23]. In addition to the

Swerling cases, the Marcum case 0 (Rayleigh-Rice distribution) for a non-fluctuating target has also been implemented for comparison with other models.

For each of these implementations it is possible to specify the number of pulses that are integrated. This can be used to model incoherent ping-to-ping integration in the sonar system or to simulate integration effectively done by the sonar operator.

4.2 Cumulative probability of detection

Section 4.1 described the method for obtaining the probability of detecting a target for a single detection opportunity (which might consist of several pings if ping-to-ping averaging is used). To provide the inputs required for MCM planning it is necessary to calculate the cumulative probability of detection (cpd). The cpd is defined here as the probability that a target at a specified lateral distance from the ship's track will be detected somewhere along that track. If statistical independence is assumed between detection opportunities, then the cpd after n detection opportunities, denoted by F_{dn} is given by:

$$F_{dn} = 1 - \prod_{i=0}^{n} (1 - p_i)$$

However, the assumption of statistical independence is generally not valid and tends to greatly over-estimate the cpd. If, on the other hand, complete dependence is assumed between detection opportunities, then F_{dn} is given by $F_{dn} = \max(p_1, p_2, \ldots, p_n)$. Reality is somewhere between these two extremes.

Wagner [37] describes a technique known as the (λ, σ) process to overcome the problem of dependence between detection opportunities. The algorithm implemented is the (λ, σ) process for the general case of discrete-glimpse search. There are three input parameters: a set of probabilities corresponding to each detection opportunity; λ; and Δ. Δ is the time between detection opportunities and λ, which has units of 1/time, is related to the correlation between detection events: $\lambda = 0$ corresponds to complete correlation, while $\lambda = \infty$ corresponds to independence between detection opportunities. The value of λ is largely empirical, Wagner quotes values of 1 and 2 per hour being used for passive ASW sonars.

4.3 Lateral range curve

Figure 2 shows the geometry used to calculate the lateral range curve (generally referred to as a $P(y)$ curve within the MCM community) for a sonar with a fixed horizontal field of view. The ship's track is along line CC and the path of the target through the sonar field of view is shown by line TT. The along-track horizontal distance from the sonar (S) to the target (P) is given by x and the across-track horizontal distance from the sonar to the target is given by y. The probability of detection is then calculated, using one of the algorithms described in section 4.1, for each detection opportunity that occurs within the sonar horizontal field of view along line TT. The cumulative probability of detection is then calculated for a target offset of y using the (λ, σ) algorithm described in section 4.2. One problem with the (λ, σ) algorithm is finding an appropriate value for λ. In the theory behind the (λ, σ) algorithm, λ is effectively the rate of change of probability events. It seems appropriate, therefore, that λ is related to the rate of change of target aspect (target strength and, therefore, probability of detection tends to vary with target aspect). In this implementation, λ is given the default value $(\delta\alpha)v/(\pi(x_{max} - x_{min}))$, where $\delta\alpha$ is the total aspect change of the target in radians, v is the ship speed, and x_{max} and x_{min} are the maximum and minimum along-track ranges of the target within the sonar horizontal field of view. In other words, λ is given the value of the proportion of a 180° aspect change that occurs on average per second. This serves as a starting point, however, λ should be adjusted in the future to fit real data. In addition to target aspect, the statistics of the environment also affect the degree of independence between detection opportunities and it may be possible to include these effects in a future algorithm to calculate λ.

Another factor that should be taken into account in producing the $P(y)$ curve is the effect that the sonar operator has on the overall probability of detection. The current implementation includes the effect of the operator by using an operator probability of detection. The system probabilities calculated at each detection opportunity are multiplied by the operator probability of detection. In reality this is a complicated human factors problem and more sophisticated algorithms to account for the operator may be added in the future.

The algorithm currently implemented for computing lateral range curves only applies to fixed horizontal field of view sonars. Algorithms applicable to sector-scan sonars and side-scan sonars will be added in the next phase of the project.

4.4 A and B_d values

The parameters characteristic detection width, A, and characteristic probability of detection, B_d, are used to characterize the $P(y)$ curve. While MCM EXPERT can use the $P(y)$ curve directly, some planning tools require the derived A and B_d values as input. Figure 3 shows an example of a $P(y)$ curve produced by ESPRESSO and the associated values of A and B_d, given by the width and height respectively of the box in the figure. One interesting feature of the $P(y)$ curve is the drop in cumulative probability of detection as the target across-track range tends toward zero. This is due to the target aspect change reducing to zero at zero across-track range causing

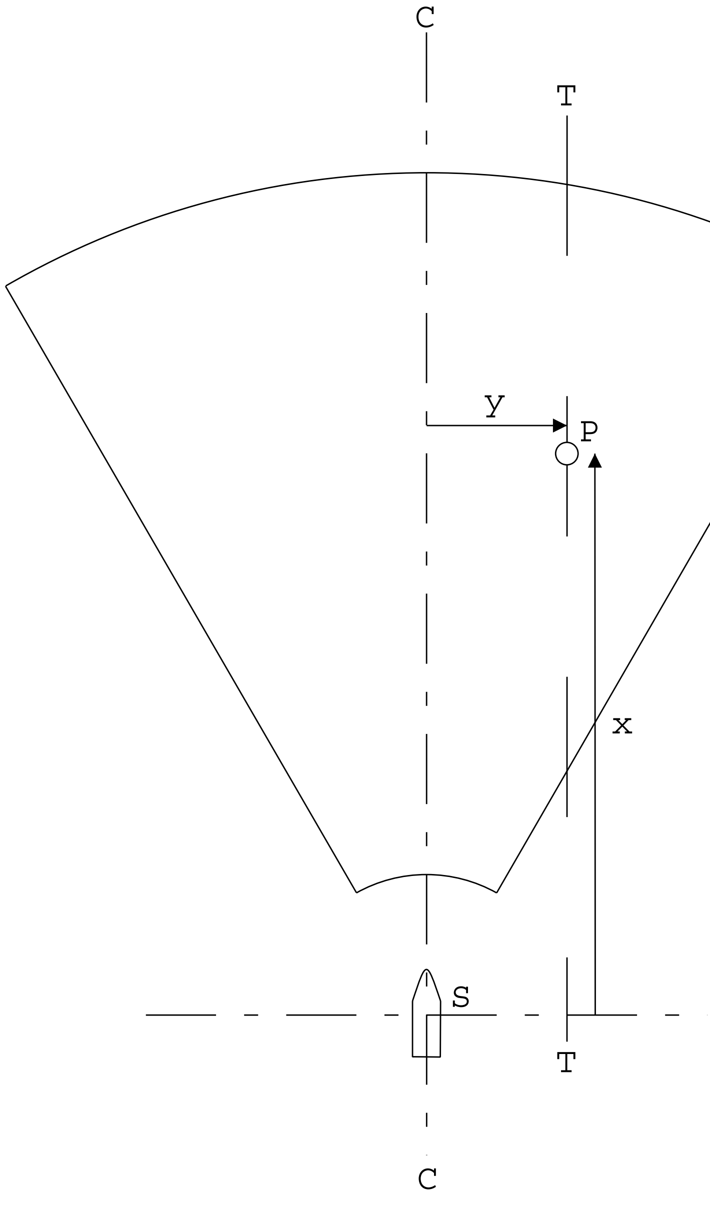

Figure 2 *Target path relative to ship*

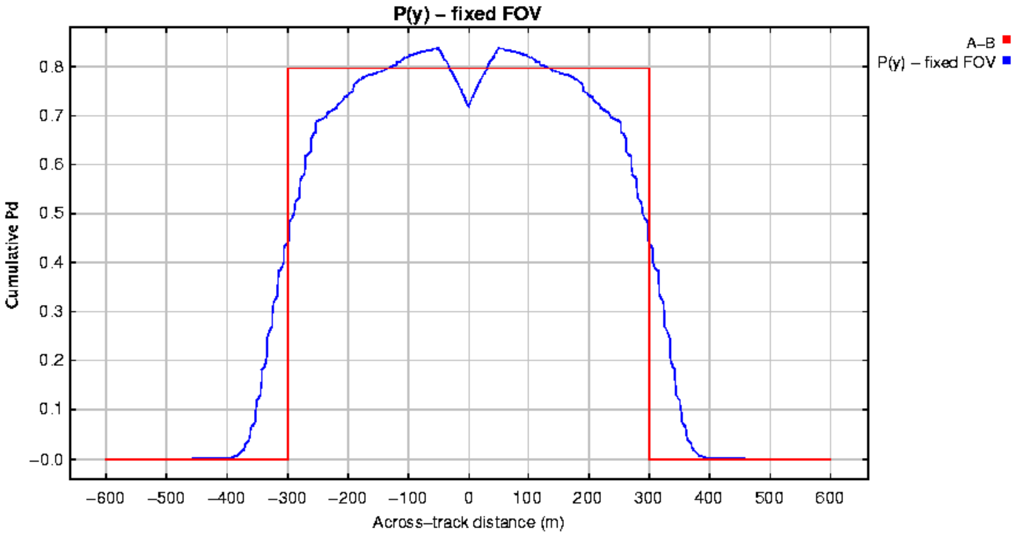

Figure 3 *A-B plot*

λ to reduce to zero, so that the cumulative probability of detection tends to the case of perfect correlation between detection opportunities. The A and B_d values are found using standard procedures [3].

5
Prototype software

A goal of the project is to deliver a tool that has the capability of being upgraded with new or improved sub-models without requiring changes or recompilation of existing code. It was not clear at the start of the project how this could be done, therefore there was significant technical risk associated with achieving this goal. It was decided, therefore, to carry out software prototyping during Phase I to develop a software architecture that would allow the goal to be achieved. A further benefit of the prototype software was that it provided a test bed for the development and testing of algorithms during Phase I.

The prototype software was written in the Java programming language. Java was chosen mainly for its platform independence and its robustness. However, another benefit of using Java is that one can then use a component technology called JavaBeans. JavaBeans technology provides mechanisms that allow applications to discover the properties and methods of a class (the building blocks of object-oriented programming). In other words, this technology can allow software to discover the input parameters required by a sub-model provided it is packaged as a JavaBean. This means that the input parameters available to the user always correspond to the input parameters of the selected sub-model. A disadvantage of Java is that its speed of execution can be slower than more conventional languages, such as C++. However, the gap between the speed of execution of Java and C++ has narrowed considerably with recent implementations of Java and it has been judged that a slight performance penalty is a price worth paying for the advantages. It is possible to add sub-models written in languages other than Java to ESPRESSO provided a Java "wrapper" is placed around the code and provided the loss of platform independence is acceptable.

Figure 4 shows the user interface provided by the prototype software for displaying parameters grouped in various categories (such as environment, sonar, etc.). This display is known as the "scenario" view since it allows the user to set up the scenario in terms of the environment, target, etc. The sub-model categories (such as bottom reflection, surface scatter, etc.) are also shown and the user can chose a sub-model from the list available within each category. As the user changes the selected sub-model for a category, the list of displayed parameters changes, if necessary, to reflect the input parameters required by the newly selected sub-model.

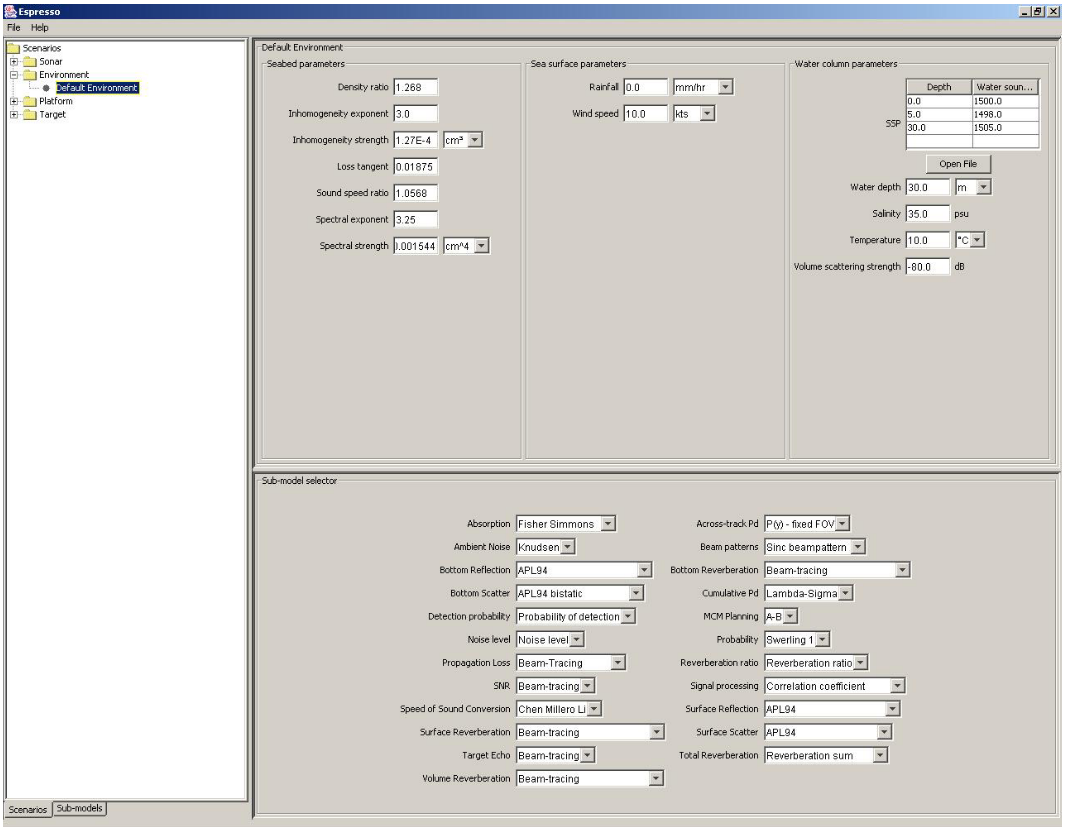

Figure 4 *User interface showing environmental parameters*

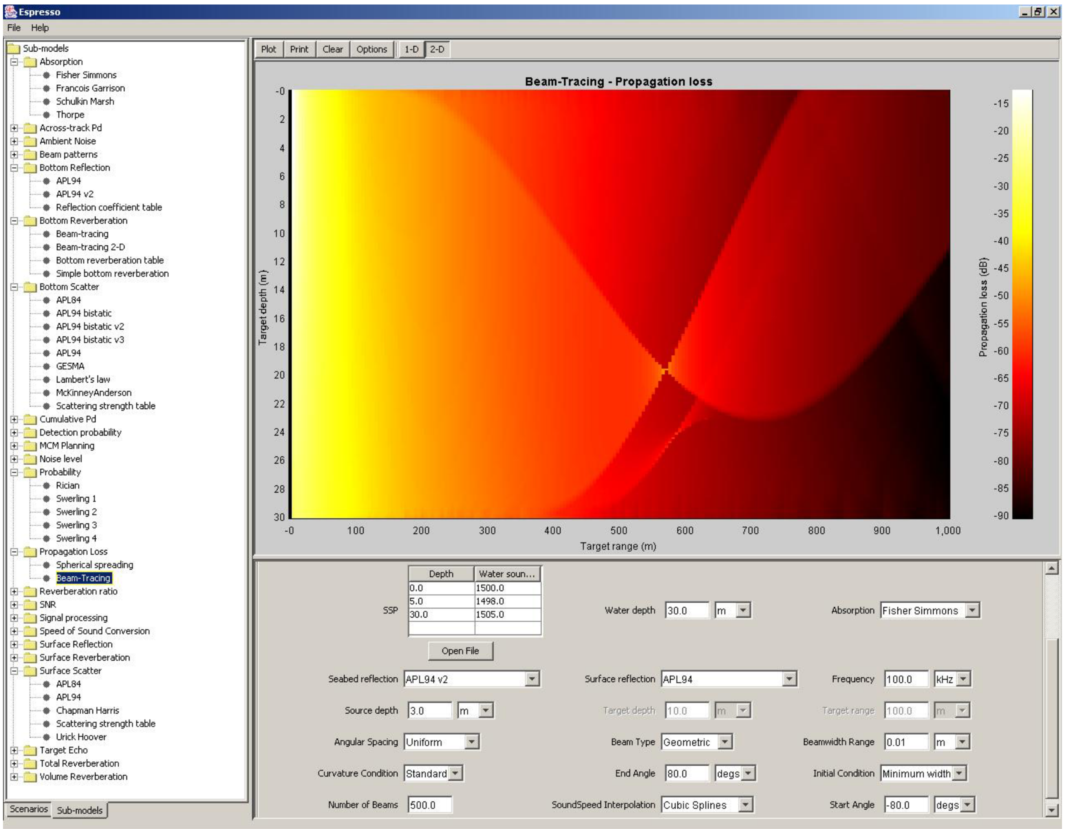

Figure 5 *User interface showing sub-models*

Figure 5 shows the user interface that the prototype software provides for displaying the results of sub-models. The sub-model is selected using the tree on the left of the display (sub-models are grouped by category). On the right of the display the user can edit the input parameters of the sub-model. The sub-model may have other dependent sub-models, for example, the propagation loss sub-model shown depends on other sub-models to calculate the bottom and surface reflection coefficients. The parameters of dependent sub-models are not shown in this display, it is necessary to select the dependent sub-model and edit its parameters there or use the scenario view described earlier. The results of the sub-model can be shown as a function of one input parameter as a line-graph or as a function of two parameters as a colour plot, as shown in the figure.

When a new sub-model gets added to ESPRESSO it automatically appears in the lists of sub-models under the appropriate sub-model category. When the new sub-model is selected from the sub-model tree, its input parameters are automatically displayed. This is achieved without requiring changes or recompilation of existing code.

The prototype software has achieved its objectives of providing a software architecture that meets the project goal defined in section 1 and has provided a test bed for algorithm development. The user interface provided by the prototype software provides the basis for an adequate user interface for scientific use, although some improvements and a user guide are needed. For military use (which is the main objective of the tool), the user interface provided by the prototype software is unsuitable. One of the main aims of the next phase of the project is to design an effective user interface for military users.

6
Remaining tasks

6.1 Implementation of ESPRESSO (Phase II)

Most of the building blocks needed for the final version of ESPRESSO have been developed as part of the software prototyping exercise, including all the essential sub-models. However, a user interface suitable for military use still needs to be designed and implemented. Once the user interface is in place, the major remaining tasks are production of the User's Guide, on-line help, and verification testing (checking the correctness of the code). ESPRESSO will then be released as a beta version. Final release of ESPRESSO will occur after validation (comparing predictions with real data and other bench-marked models), which will include the use of results from Percentage Clearance (PC) trials (see section 6.3). Other tasks include integration of improved sub-models, such as seabed scattering and target scattering sub-models being developed by other projects at SACLANTCEN.

6.2 Verification

All the sub-models implemented so far have undergone some verification. In most cases, sub-models have been verified by comparing the output of the implemented sub-model with documented results (for example, those provided by APL-UW in [2]). In other cases, where code has been available in FORTRAN or MATLAB, the results of the Java implementation have been compared with results from the code provided (the propagation loss and mine burial sub-models were verified in this way).

For the sub-models developed specifically for ESPRESSO at SACLANTCEN, verification has been done by comparing results with analytic cases. Meyer and Davies [25] provide comparisons of results of the reverberation sub-models with analytic cases. Verification of ESPRESSO will continue during both Phases II and III.

6.3 Validation (Phase III)

Where sub-models have been developed outside Project 03F-1, it is assumed that these sub-models are already validated. It is beyond the scope of Project 03F-1 to

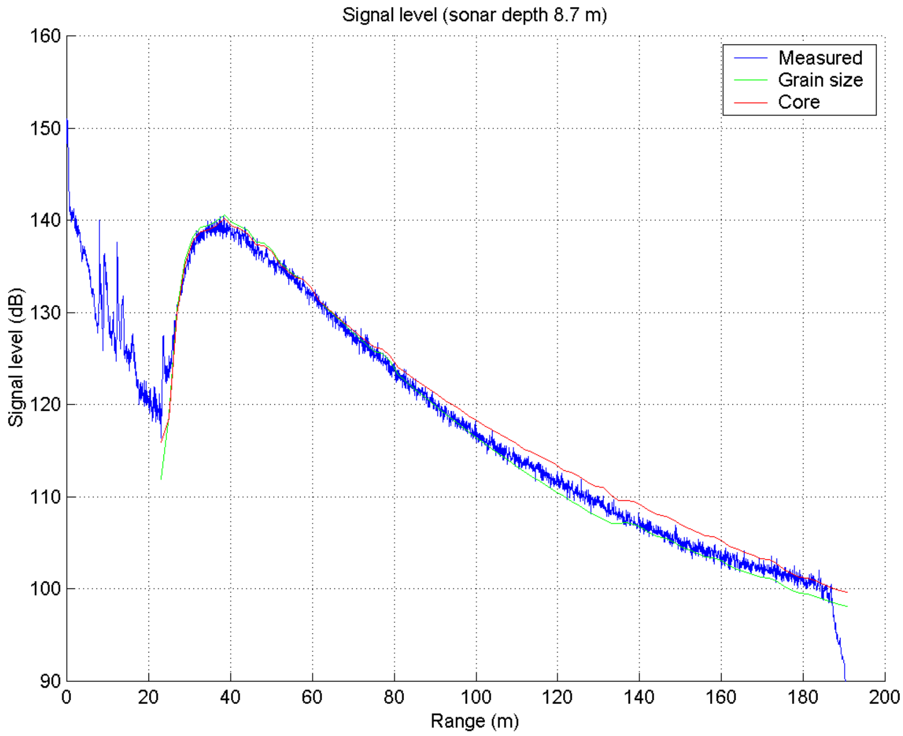

Figure 6 *Comparison of ESPRESSO predictions with data*

carry out further validation of these sub-models, even in cases where they may be used outside the limits of their validation. As an example, although there are ongoing efforts to validate the APL-UW 1994 bottom scattering sub-model at frequencies above 100 kHz, until this has been done it will be necessary to use this sub-model outside the limits of its current validation for sonars operating above 100 kHz because no better alternative sub-model is available.

Sub-models that have been developed within the project (in particular, the reverberation sub-models) will be validated during the course of the project. Some comparisons have been done by Wang et al. [38] between data collected in the MASAI '01 cruise and predictions of reverberation levels by ESPRESSO. These comparisons showed good agreement after the seabed volume scattering coefficient had been adjusted to match the measured seabed backscattering strength. Figure 6 shows a comparison between the ESPRESSO predictions using seabed properties taken from core samples (red line) and derived from the mean grain size (green line) with measured data from the MASAI '01 cruise (blue line).

Data collected during the MASAI '02 cruise should allow more detailed testing of the reverberation sub-models. These data were collected using a vertical array allowing

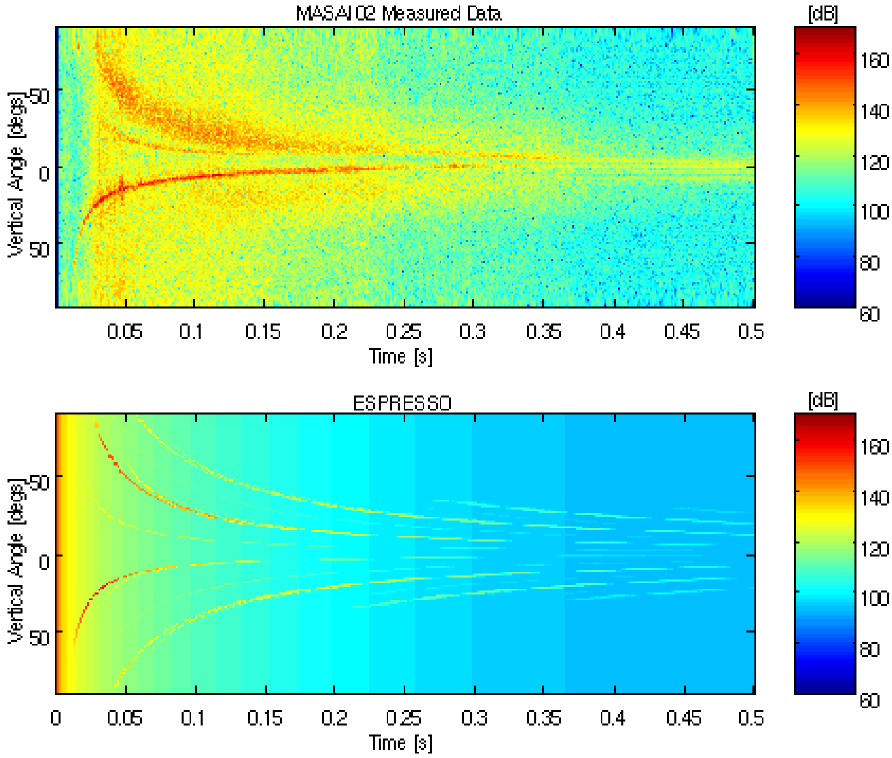

Figure 7 *Reverberation versus vertical arrival angle and time*

the various reverberation multipaths to be distinguished (by vertical arrival angle and travel time). Figure 7 gives an example of reverberation data from the MASAI '02 cruise together with the ESPRESSO prediction of reverberation intensity versus vertical arrival angle and time. Comparing the predicted and measured data there are clearly some differences; in particular, the spread of reverberation energy over vertical angle seen in the measured data for paths that have undergone sea surface reflections does not appear in the predicted data. Further comparisons between ESPRESSO and the MASAI '02 data will be done during the project and these may lead to some improvements in the fidelity of ESPRESSO.

ESPRESSO will also be benchmarked against the CASS model, a model that has itself been benchmarked against a number of other models, to test it over a variety of environments. Figure 8 is an example of predictions by ESPRESSO (red line) and CASS (blue line) using input parameters representative of one of the experiments held during the MASAI '02 trial.

The most difficult (but the most important, from a military perspective) part of ESPRESSO to validate is the lateral range curve ($P(y)$ curve) prediction. The

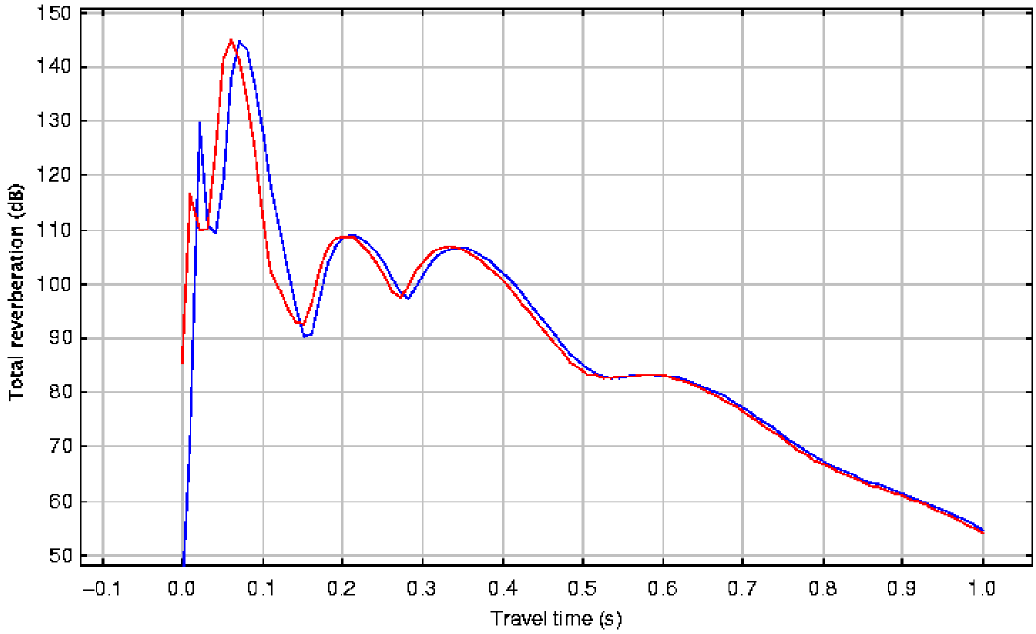

Figure 8 *Benchmarking against CASS*

difficulty is in designing a controlled experiment where the factors affecting the $P(y)$ curve are sufficiently well known. The intention is to compare the results of Percentage Clearance (PC) trials during Phase III with predictions by ESPRESSO. These, however, are some of the problems with this approach:

- Sonar operator efficiency difficult to quantify
- Detailed knowledge of sonar parameters required (e.g. beampatterns)
- Detailed knowledge of the environment required (e.g. seabed characteristics)
- Characteristics of targets needed (e.g. target strength)
- Statistically significant number of targets needed

With the degree of uncertainty of the factors affecting sonar performance, an exact match between measured and predicted $P(y)$ curves cannot be expected. However, it is hoped that it will be possible to demonstrate that ESPRESSO can provide a significant improvement in the prediction of sonar performance compared to predictions made using current methods. These trials will also provide an opportunity to define more appropriate values for the operator probability of detection and for λ, described in section 4.3.

7 Conclusion

Phase I of Project 03F-1 achieved its objectives of minimizing technical risk and developing the essential sub-models needed to predict sonar performance. The prototype software resulting from Phase I can be used as a scientific tool, with the proviso that it has not yet been extensively validated. Many of the building blocks are in place for producing the beta release of ESPRESSO, although a suitable user interface still needs to be designed and implemented.

References

[1] APL-UW Ocean environmental acoustic models. Technical Report APL-UW 8407, Applied Physics Laboratory, University of Washington, 1013 NE 40th Street, Seattle, WA 98105-6698, June 1984.

[2] APL-UW High-frequency ocean environmental acoustic models handbook. Technical Report APL-UW TR 9407, Applied Physics Laboratory, University of Washington, 1013 NE 40th Street, Seattle, WA 98105-6698, October 1994.

[3] ATP6(B). NATO Tactical Publication.

[4] P. Caprais and A. Lombardi. Development of a SACLANTCEN MCM sonar performance model. SACLANTCEN Memorandum SM-315, SACLANT Undersea Research Centre, November 1996.

[5] R. P. Chapman and J. H. Harris. Surface backscattering strength measured with explosive sound sources. *Journal of the Acoustical Society of America*, 34:1592–1597, 1962.

[6] C. Chen and F. J. Millero. Re-evaluation of Wilson's soundspeed measurements in pure water. *Journal of the Acoustical Society of America*, 60:1270–1273, 1976.

[7] C. Chen and F. J. Millero. Speed of sound in seawater at high pressures. *Journal of the Acoustical Society of America*, 62:1129–1135, 1977.

[8] P. A. Crowther. Acoustical scattering from near-surface bubble layers. In W. Lauterborn, editor, *Cavitation and Inhomogeneities in Underwater Acoustics*, pages 195–204. Springer-Verlag, New York, 1980.

[9] P. H. Dahl. Revisions and notes on a model for bubble attenuation in near-surface acoustic propagation. Technical Report APL-UW TR 9411, Applied Physics Laboratory, University of Washington, 1013 NE 40th Street, Seattle, WA 98105-6698, July 1994.

[10] Peter H. Dahl. On bistatic sea surface scattering: Field measurements and modeling. *Journal of the Acoustical Society of America*, 105:2155–2169, April 1999.

[11] T. Edgecock. High frequency warm sea water sound absorption. In *UDT*, pages 423–427, 1994.

[12] F. H. Fisher and V. P. Simmons. Sound absorption in sea water. *Journal of the Acoustical Society of America*, 62:558–56, 1977.

[13] R. E. Francois and G. R. Garrison. Sound absorption based on ocean measurements. part I: Pure water and magnesium sulfate contributions; part II: Boric acid contribution and equation for total absorption. *Journal of the Acoustical Society of America*, 72:896–907,1879–1890, 1982.

[14] G. J. Franz. Splashes as sources of sound in liquids. *Journal of the Acoustical Society of America*, 1959.

[15] R. Keenan, H. Weinberg, and F. Aidala. Software requirements specification, GRAB: Gaussian ray bundle eigenray propagation model. Technical report, Naval Oceanographic Office, 1997.

[16] V. O. Knudsen, R. S. Alford, and J. W. Emling. Underwater ambient noise. *J. Marine Research*, 7:410–429, 1948. Reprinted in "Underwater Sound - Benchmark Papers in Acoustics" by V. M. Albers, 1972.

[17] Y. C. Liu and M. B. Porter. Geometric beam tracing. *Journal of the Acoustical Society of America*, 92:2372–2373, 1992.

[18] K. V. Mackenzie. Reflection of sound from coastal bottoms. *Journal of the Acoustical Society of America*, 32:221–231, 1959.

[19] K. V. Mackenzie. Bottom reverberation for 503- and 1030-cps sound in deep water. *Journal of the Acoustical Society of America*, 33(11):1498–1504, 1961.

[20] S. T. McDaniel. Sea surface reverberation: A review. *Journal of the Acoustical Society of America*, 94:1905–1922, 1993.

[21] S. T. McDaniel and A. D. Gorman. Acoustic and radar sea-surface backscatter. *J. Geophys. Res.*, 87:4127–4136, 1982.

[22] C. M. McKinney and C. D. Anderson. Measurements of backscattering of sound from the ocean bottom. *Journal of the Acoustical Society of America*, 36:158–163, 1964.

[23] Daniel P. Meyer and Herbert A. Mayer. *Radar Target Detection: Handbook of Theory and Practice.* Academic Press, 1973.

[24] M. Meyer and G. L. Davies. Application of the method of geometric beam tracing for high frequency reverberation modelling. In *Acta Acustica united with Acustica*, number 5. 2002. Accepted paper.

[25] M. Meyer and G. L. Davies. A beam-based high frequency reverberation model. Technical Report SR-365, SACLANT Undersea Research Centre, 2002.

[26] M. Meyer and G. L. Davies. Beam tracing techniques for high frequency reverberation modelling. In *Proceedings of the 6th European Conference on Underwater Acoustics*, Gdansk, 2002.

[27] F. J. Millero and X. Li. Comments on 'on equations for the speed of sound in seawater'. *Journal of the Acoustical Society of America*, 95:2757–2759, 1994.

[28] P. D. Mourad and D. R. Jackson. High frequency sonar equation models for bottom backscatter and forward loss. In *Proceeding of OCEANS '89*, pages 1168–1175. Marine Technology Society and IEEE, 1989.

[29] M. Porter. The kraken normal mode program. SACLANTCEN Memorandum SM-245, SACLANT Undersea Research Centre, September 1991.

[30] M. B. Porter and H. P. Bucker. Gaussian beam tracing for computing ocean acoustic fields. *Journal of the Acoustical Society of America*, 82(4):1349–1359, 1987.

[31] T. Sakai, K. Hatanaka, and H. Mase. Wave induced stresses in seabed and its momentary liquefaction. In *Proc. ASCE, J. Waterways, Port, Coastal and Ocean Engineering*, volume 118(WW2), pages 202–206, 1992.

[32] M. Schulkin and H. W. Marsh. Sound absorption in sea water. *Journal of the Acoustical Society of America*, 34:864–865, 1962.

[33] Mine burial prediction, subgroup 31 analysis and final report. Technical report, SG-31, June 1999.

[34] W. H. Thorp. Deep-ocean sound attenuation in the sub-and low-kilocycle-per-second-region. *Journal of the Acoustical Society of America*, 38:648–654, 1965.

[35] E. I. Thorsos. Surface forward scattering and reflection. Technical Report APL-UW 7-83, Applied Physics Laboratory, University of Washington, 1013 NE 40th Street, Seattle, WA 98105-6698, May 1984.

[36] R. J. Urick and R. M. Hoover. Backscattering of sound from the sea surface. *Journal of the Acoustical Society of America*, 28:1038–1042, 1956.

[37] Daniel H. Wagner, W. Charles Mylander, and Thomas J. Sanders, editors. *Naval Operations Analysis*, chapter 5. Number ISBN 1-55750-956-5. Naval Institute Press, Annapolis, 3rd edition, 1999.

[38] L. Wang, G. Davies, A. Bellettini, and M. Pinto. Multipath effect on DPCA micronavigation of a synthetic aperture sonar. In N. Pace and F. Jensen, editors, *Impact of Littoral Environmental Variability on Acoustic Predictions and Sonar Performance*, pages 465–472. Kluwer Academic, September 2002.